JOURNAL OF MATERIALS SCIENCE 18 (1983) 3259–3264

Thermal conductivity of chemically vapour-deposited Si_3N_4–TiN composites

SHINSUKE HAYASHI, TOSHIO HIRAI
The Research Institute for Iron, Steel and Other Metals, Tohoku University, Sendai 980, Japan

The thermal conductivity of Si_3N_4–TiN composites with TiN dispersed uniformly in the Si_3N_4 matrix prepared by CVD of a $SiCl_4$–$TiCl_4$–NH_3–H_2 system was measured at the temperature range of 20 to 900° C. The conductivity of composites having the crystalline Si_3N_4 matrix decreased drastically with increase in the TiN content and was markedly different from the values calculated using the general mixture rule. This phenomenon results from the peculiar microstructure of the Si_3N_4–TiN composites.

1. Introduction

Silicon nitride is promising as a structural material since it has high strength and superior resistance to creep, corrosion and oxidation. Thermal shock resistance is one of the important properties for high temperature applications and is closely related to thermal conductivity. Because the thermal conductivity is structure sensitive, especially for ceramics, the effects of microstructures on the thermal conductivity of Si_3N_4 bodies have been examined [1–8].

We have prepared Si_3N_4–TiN composites by CVD of a $SiCl_4$–$TiCl_4$–NH_3–H_2 system and have previously reported the crystal structure, preferred orientation, surface morphology, TiN content and microstructure [9–12]. The present study was conducted to clarify the effects of the composition and microstructure on the thermal conductivity of these Si_3N_4–TiN composites.

2. Experimental procedure

2.1. Sample preparation

The Si_3N_4–TiN composites were deposited on a directly heated graphite substrate at deposition temperatures (T_{dep}) of 1050 to 1450° C and total gas pressures (P_{tot}) of 1.33 to 10.7 kPa using $SiCl_4$, $TiCl_4$, NH_3 and H_2 gases. The flow rates of $SiCl_4$, $TiCl_4$, NH_3 and H_2 were 136, 18, 120 and 2720 $cm^3 min^{-1}$, respectively. The details of the sample preparation were previously reported [11]. As shown in Table I, the structure of the Si_3N_4 matrix and the TiN content depended on T_{dep} and P_{tot}. The composites having amorphous, α- and β-Si_3N_4 matrices are designated as amorphous, α- and β-composites, respectively, in the following text. The TiN was deposited in the form of NaCl type crystal.

2.2. Thermal conductivity measurement

A disc 5 mm in diameter and 0.5 to 1.5 mm in thickness was cut out from the deposits. The thermal diffusivity (α) was measured by means of the laser flash method; details were previously reported [6]. The specific heat of the composites (C_p) was determined from the reported values of the specific heats of Si_3N_4 [6] and TiN [13] and the TiN content. The thermal conductivity (k) was calculated using Equation 1.

$$k = \alpha C_p \rho. \qquad (1)$$

Here ρ is the density of the composites.

3. Results and discussion

Figs. 1 to 4 give the thermal conductivity (k) of the composites prepared at P_{tot} of 1.33 to 10.7 kPa. It is clear that the conductivity of α- and β-composites is higher than that of the amorphous composites. The α- and β-composites exhibited a negative temperature dependence of k, which is typical of crystalline dielectric ceramics such as Si_3N_3. However, this temperature dependence for the composites was not as strong as that observed for the

0022–2461/83 $03.00 + .12

TABLE I Preparation conditions and some properties of Si_3N_4–TiN composites

Deposition temperature T_{dep}(° C)	Total gas pressure, P_{tot}(kPa)	TiN volume fracture	Structure of the Si_3N_4 matrix*	Density of the Si_3N_4 matrix (g cm^{-3})
1050	4	0.192	Am	2.85
1050	8	0.095	Am	2.92
1150	1.33	0.199	Am	2.86
1150	4	0.051	Am	3.03
1150	8	0.052	Am	3.02
1150	10.7	0.045	Am	2.92
1250	1.33	0.062	α	3.18
1250	4	0.027	α	3.19
1250	8	0.024	α	3.15
1250	10.7	0.026	Am	2.96
1350	1.33	0.044	α	3.17
1350	4	0.026	β	3.18
1350	8	0.021	β	3.17
1350	10.7	0.021	β	3.18
1450	1.33	0.046	β	3.15
1450	4	0.021	β	3.20
1450	8	0.016	β	3.18
1450	10.7	0.020	β	3.18

*Am: amorphous Si_3N_4, α: α-Si_3N_4, β: β-Si_3N_4.

pure α-Si_3N_4, which exhibited a marked decrease in k from 59 W m^{-1} K^{-1} at 20° C to 22 W m^{-1} K^{-1} at 900° C [6]. TiN is an electric conductor and the thermal conductivity slightly increased from 21 W m^{-1} K^{-1} at 20° C to 25 W m^{-1} K^{-1} at 900° C [14]. The amorphous composites exhibited a weak positive temperature dependence of k, which is typical of amorphous ceramics.

As shown in Table I, the density of the crystalline Si_3N_4 matrix was independent of preparation conditions and almost equal to the theoretical values of 3.18 g cm^{-3} for α-Si_3N_4 and 3.19 g cm^{-3} for β-Si_3N_4 [15]. On the contrary, the density of the amorphous Si_3N_4 matrix varied from 2.85 to 3.03 g cm^{-3}, depending on T_{dep} and P_{tot}. The dependence of k on the density of the amorphous

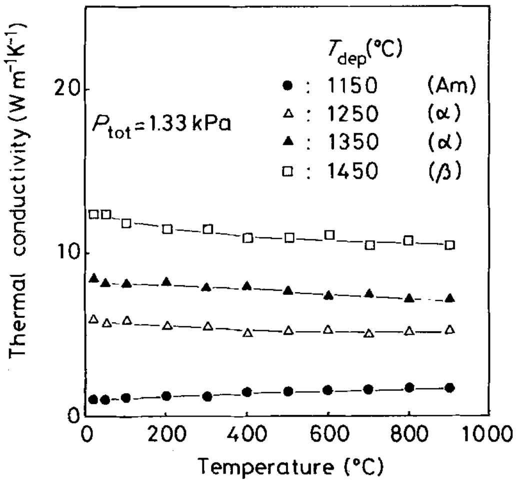

Figure 1 Thermal conductivity of the Si_3N_4–TiN composites prepared at P_{tot} of 1.33 kPa.

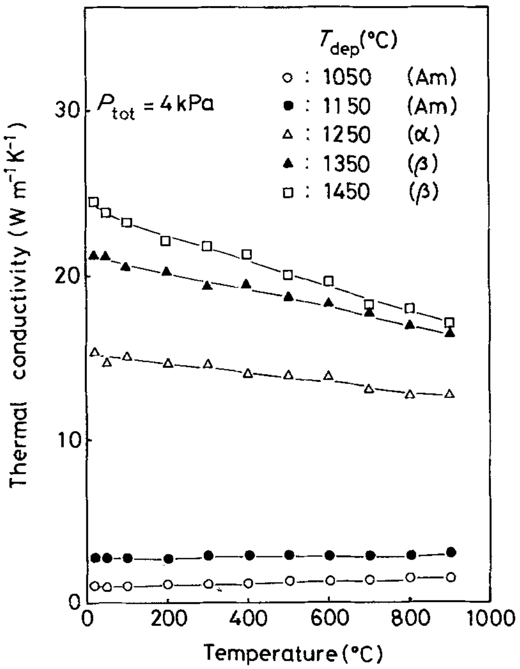

Figure 2 Thermal conductivity of the Si_3N_4–TiN composites prepared at P_{tot} of 4 kPa.

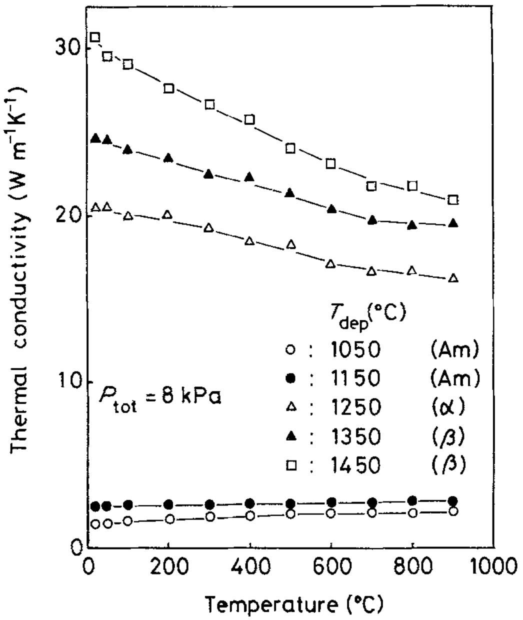

Figure 3 Thermal conductivity of the Si_3N_4–TiN composites prepared at P_{tot} of 8 kPa.

Si_3N_4 matrix was examined. However, no clear relationship between them was found.

Figs. 5 and 6 show the relationship between the composition and k at 20 and 900° C, respectively. Here, the conductivities for the amorphous and α-Si_3N_4 at the zero TiN volume fraction are the previously reported values on CVD-Si_3N_4 [6]. Pure β-Si_3N_4 has not yet been prepared by CVD.

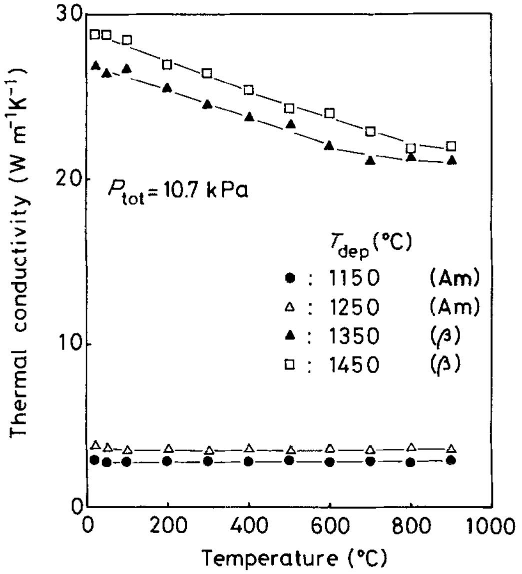

Figure 4 Thermal conductivity of the Si_3N_4–TiN composites prepared at P_{tot} 10.7 kPa.

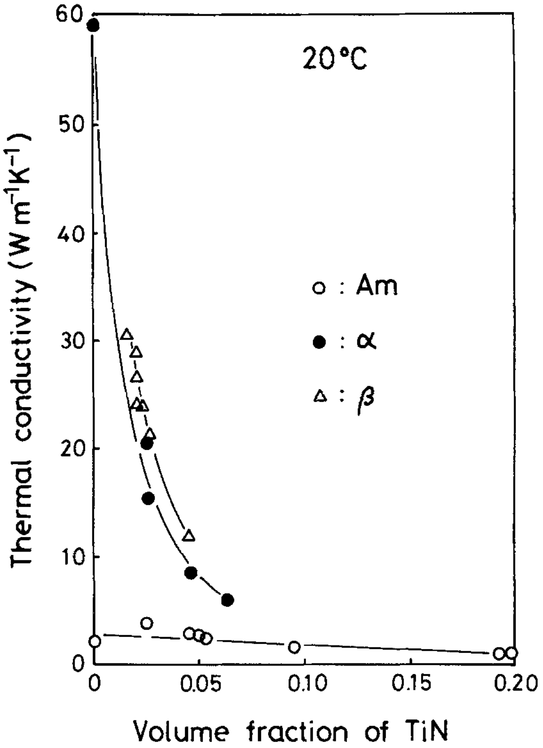

Figure 5 Relationship between the thermal conductivity at 20° C of the Si_3N_4–TiN composites and the TiN volume fraction.

For amorphous composites, the conductivity decreased slightly with increasing TiN volume fraction. A similar phenomenon has been observed in Si_3N_4–C composites with carbon dispersed in the amorphous Si_3N_4 matrix prepared by CVD

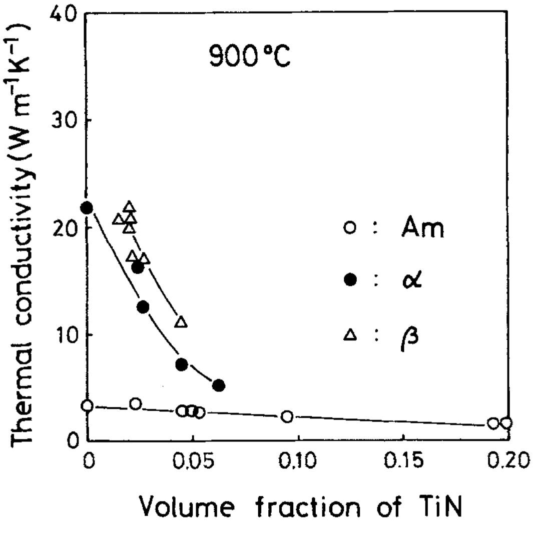

Figure 6 Relationship between the thermal conductivity at 900° C of the Si_3N_4–TiN composites and the TiN volume fraction.

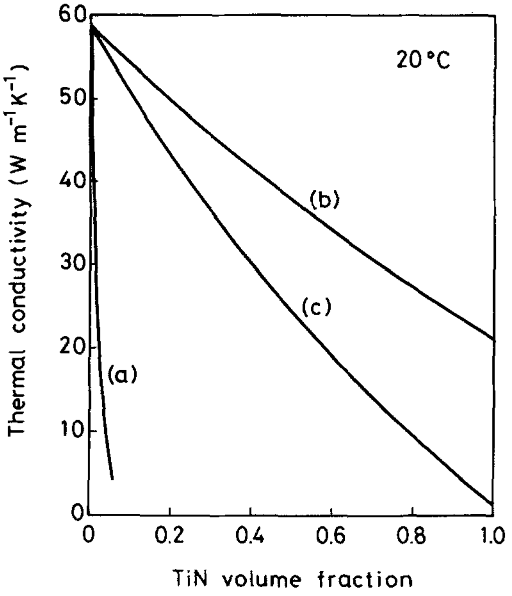

Figure 7 Comparison of the thermal conductivity of the α-composites measured at 20° C with the theoretical. (a) measured curve, (b) theoretical curve for 21 W m^{-1} K^{-1} of the TiN conductivity, (c) theoretical curve for 1.2 W m^{-1} K^{-1} of the TiN conductivity.

of a $SiCl_4$–NH_3–H_2–C_3H_8 system [16]; the increase in the carbon content caused the decrease in the conductivity of the Si_3N_4–C composites.

For the α- and β-composites, two results must be pointed out. One is the drastic decrease in the conductivity with increasing TiN volume fraction; the conductivity at 20° C of the α-composite with 0.062 TiN volume fraction is about one tenth in magnitude of that of the pure α-Si_3N_4. A detailed discussion about this phenomenon is described later. The second point is that the β-composites exhibited high conductivity compared to α-composites. Tsukuma *et al.* [7] obtained a pure β-Si_3N_4 body with a density of 3.15 g cm^{-3} by high pressure hot-pressing using no additives and reported the room temperature conductivity to be 30 W m^{-1} K^{-1}. This value is low compared to that of α-Si_3N_4 prepared by CVD [6]. Ziegler and Hasselman [8] stated that the conductivity of α-Si_3N_4 is lower than that of β-Si_3N_4 because of the more strained crystal structure of the α-phase compared to the β-phase. As previously reported [12], the microstructure of the β-composites is different from that of the α-composites; while the TiN in the β-Si_3N_4 matrix is columnar, that in the α-Si_3N_4 matrix is particulate. However, the TiN dispersions in the both matrices are contained in Si_3N_4 crystal grains. Although the shape of the TiN dispersions may have an influence on the conductivity, the results shown in Figs. 5 and 6 seem to support Ziegler's statement.

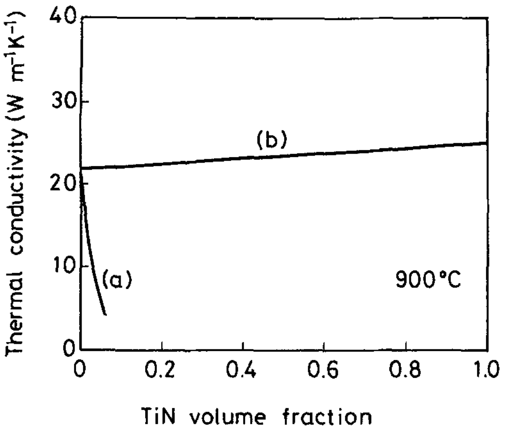

Figure 8 Comparison of the thermal conductivity of the α-composites measured at 900° C with the theoretical. (a) measured curve, (b) theoretical curve for 25 W m^{-1} K^{-1} of the TiN conductivity.

For a composite with spherical inclusions dispersed uniformly in the matrix, the Equation 2 is proposed to estimate the thermal conductivity of the composite [17].

$$k_c = k_m \frac{1 + 2V_d(1 - k_m/k_d)/(2k_m/k_d + 1)}{1 - V_d(1 - k_m/k_d)/(2k_m/k_d + 1)}. \tag{2}$$

Here, k_c, k_m and k_d are the conductivities of the composite, matrix and dispersion, respectively, and V_d is the volume fraction of the dispersion. Lange [2] measured the room temperature conductivity of Si_3N_4–SiC composites containing 0.1 to 0.4 volume fraction of the SiC dispersions which were fabricated from powder mixtures of α-Si_3N_4, MgO and SiC with average sizes of 5 to 32 μm. He observed a predicted increase in the conductivity with the SiC addition and a fairly good agreement of the measured values with those calculated from Equation 2.

Figs. 7 and 8 show comparisons of the conductivity of the α-composites measured at 20 and 900° C, respectively, with the theoretical values from Equation 2. The conductivity of TiN is the reported values, 21 W m^{-1} K^{-1} at 20° C and 25 W m^{-1} K^{-1} at 900° C [14]. It is apparent from Figs. 7 and 8 that measured values are markedly different from the theoretical and some α-composites exhibited lower conductivities than those of the end members, α-Si_3N_4 and TiN.

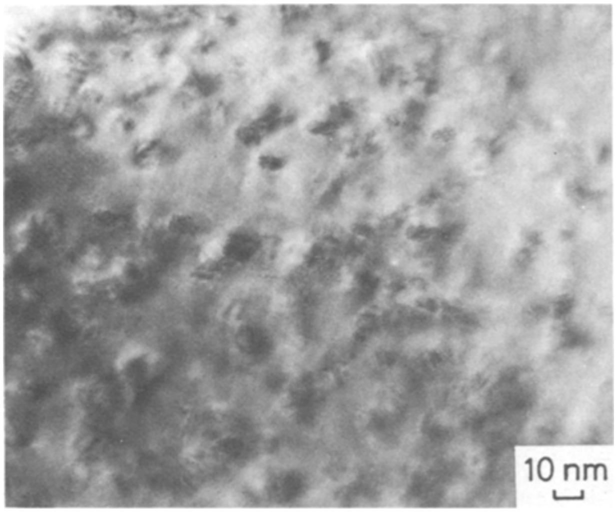

Figure 9 Electron micrograph of the α-composite prepared at T_{dep} of 1250° C and P_{tot} of 4 kPa.

In solids, heat is mainly transmitted via phonons for dielectrics and electrons for conductors. Besides phonon–phonon, electron–phonon and electron–electron collisions, imperfections in solids also act as scattering centres for phonons and electrons, becoming sources of the thermal resistance. The impurity atoms, dislocations, grain boundaries, pore, etc. are included in imperfections.

Yamada *et al.* [18] measured the room temperature thermal conductivity of TiN bodies prepared by high pressure hot-pressing and found a grain size dependence of the conductivity (k_{T}/W m^{-1} K^{-1}) in the grain size (d/m) range of 0.3 to 20 μm, as written in Equation 3.

$$k_{\mathrm{T}} = 8.0 \times (d \times 10^{6})^{0.41}. \qquad (3)$$

They stated that the scattering of electrons at the grain boundaries is related to the variation of the conductivity.

As shown in Fig. 9, the TiN in the α-composites is uniformly dispersed; however, the size is as small as about ten nanometres. Using Equation 3, k_{T} at d of 10 nm is estimated to be 1.2 W m^{-1} K^{-1}. In Fig. 7, the theoretical curve calculated using the value 1.2 W m^{-1} K^{-1} is also drawn. However, this does not agree with the measured values; additional sources of the thermal resistance may exist. As previously described, the TiN dispersions are included in the Si_3N_4 grains. Such an inclusion distorts the crystal lattice of Si_3N_4 and may generate dislocations and subboundaries in the crystal [19]. These imperfections are thought to act as additional scattering centres for phonons, causing the decrease in the conductivity.

4. Conclusions

(a) The α- and β-composites exhibited a negative temperature dependence of the thermal conductivity, while the amorphous composites exhibited a positive temperature dependence.

(b) The conductivity of the amorphous composites decreased slightly with increase in the TiN content.

(c) The conductivity of the β-composites was higher than that of the α-composites.

(d) The conductivity of the α- and β-composites decreased drastically with increase in the TiN content and was markedly different from the theoretical values calculated using the general mixture rule.

Acknowledgement

The authors wish to express their appreciation to Mr A. Ohkubo (RIISOM, Tohoku University) for his assistance in preparing the test samples.

References

1. W. GEORGE, *Proc. Brit. Ceram. Soc.* **22** (1973) 147.
2. F. F. LANGE, *J. Amer. Ceram. Soc.* **56** (1973) 445.
3. R. R. WILLS, R. W. STEWART and J. M. WIMMER, *Amer. Ceram. Soc. Bull.* **55** (1976) 975.
4. M. KURIYAMA, Y. INOMATA, T. KIJIMA and Y. HASEGAWA, *ibid.* **57** (1978) 1119.
5. W. ZDANIEWSKI, D. P. H. HASSELMAN, H. KNOCH and J. HEINRICH, *ibid.* **58** (1979) 539.
6. T. HARAI, S. HAYASHI and K. NIIHARA, *ibid.* **57** (1978) 1126.
7. K. TSUKUMA, M. SHIMADA and M. KOIZUMI, *ibid.* **60** (1981) 910.
8. G. ZIEGLER and D. P. H. HASSELMAN, *J. Mater. Sci.* **16** (1981) 495.

9. T. HIRAI and S. HAYASHI, *Commun. Amer. Ceram. Soc.* 64 (1981) C-88.
10. *Idem*, in Proceedings of the 8th International Conference on Chemical Vapor Deposition, Gouvieux-Chantilly, September 1981, edited by J. M. Blocher, Jr, G. E. Vuillard and G. Wahl (Electrochemical Society, Pennington, 1981) p. 790.
11. *Idem, J. Mater. Sci.* 17 (1982) 1320.
12. S. HAYASHI, T. HIRAI, K. HIRAGA and M. HIRABAYASHI, *ibid.* 17 (1982) 3336.
13. B. F. NAYLOR, *J. Amer. Chem. Soc.* 68 (1946) 370.
14. R. PORAT, in Proceedings of the 8th International Conference on Chemical Vapor Deposition, Gouvieux-Chantilly, September 1981, edited by J. M. Blocher, Jr., G. E. Vuillard and G. Wahl (Electrochemical Society, Pennington, 1981) p. 533.
15. S. WILD, P. GRIEVESON and K. H. JACK, in "Special Ceramics 5", edited by P. Popper (British Ceramic Research Association, Stoke-on-Trent, 1972) p. 385.
16. T. GOTO, S. HAYASHI and T. HIRAI, *Sci. Rep. RITU* A-29 (1981) 176.
17. W. D. KINGERY, *J. Amer. Ceram. Soc.* 42 (1959) 617.
18. T. YAMADA, M. SHIMADA and M. KOIZUMI, *Amer. Ceram. Soc. Bull.* 59 (1980) 611.
19. K. HIRAGA, M. HIRABAYASHI, S. HAYASHI and T. HIRAI, submitted to *J. Amer. Ceram. Soc.*

Received 21 February
and accepted 1 March 1983